Research Repository UCD

Title	The optimisation of dye sensitised solar cell working electrodes for graphene and SWCNTs containing quasi-solid state electrolytes
Authors(s)	Byrne, Owen, Ahmad, Iftikhar, Surolia, Praveen K., Thampi, Ravindranathan, et al.
Publication date	2014-12
Publication information	Byrne, Owen, Iftikhar Ahmad, Praveen K. Surolia, Ravindranathan Thampi, and et al. “The Optimisation of Dye Sensitised Solar Cell Working Electrodes for Graphene and SWCNTs Containing Quasi-Solid State Electrolytes.” Elsevier, December 2014. https://doi.org/10.1016/j.solener.2014.09.018.
Publisher	Elsevier
Item record/more information	http://hdl.handle.net/10197/6108
Publisher's statement	This is the author’s version of a work that was accepted for publication in Solar Energy. Changes resulting from the publishing process, such as peer review, editing, corrections, structural formatting, and other quality control mechanisms may not be reflected in this document. Changes may have been made to this work since it was submitted for publication. A definitive version was subsequently published in Solar Energy (VOL 110, ISSUE 2014, (2014)) DOI: 10.1016/j.solener.2014.09.018
Publisher's version (DOI)	10.1016/j.solener.2014.09.018

Downloaded 2026-05-01 23:36:11

The UCD community has made this article openly available. Please share how this access benefits you. Your story matters! (@ucd_oa)

© Some rights reserved. For more information

The optimisation of dye sensitised solar cell working electrodes for graphene and SWCNTs containing quasi-solid state electrolytes

Owen Byrne[a,1], Iftikhar Ahmad[b,1], Praveen K. Surolia[a], Yurii K. Gun'ko [b,c]*, K. R. Thampi[a]*.

Highlights

- Graphene & CNT based quasi-solid state electrolytes for dye sensitised solar cells.
- Charge transfer resistances at counter electrode reduced by almost a factor of 50.
- Optimisation of DSSC working electrodes for quasi-solid state electrolytes.
- Significant performance improvement for quasi-solid state DSSC is achieved.

Abstract

In this study, we report improved power conversion efficiencies of various carbon based quasi-solid state electrolytes/DSSCs by optimising the thickness of TiO_2 layer, incorporation of TiO_2 scattering layer and application of dense compact surface layers of TiO_2 on working electrodes. Single wall carbon nanotube (SWCNT) based quasi-solid state electrolytes showed increased power conversion efficiencies from 1.43 % to 3.49 %. For the mixture of graphene and SWCNTs the power conversion efficiencies improved from 2.50 % to 2.93 %. However, graphene based quasi-solid state electrolytes displayed small decreases in power conversion efficiencies from 2.10 % to 1.96 % due to the more viscous nature of this electrolyte. Electrochemical Impedance Spectroscopy (EIS) demonstrated that the addition of these various carbon based nanomaterials into PMII significantly decreases the charge transfer resistance at the counter electrode and hence the much better performance obtained with carbon based quasi-solid state electrolytes compared to pure PMII based DSSCs.

Keywords: quasi-solid state electrolyte; graphene; SWCNT; dye sensitised solar cells; photovoltaics.

[a] SFI Strategic Research Cluster in Solar Energy Conversion, UCD School of Chemical & Bioprocess Engineering, University College Dublin, Ireland.
E-mail: ravindranathan.thampi@ucd.ie, Tel: +353-1-7161995.

[b] School of Chemistry and CRANN, Trinity College Dublin, Dublin 2, Ireland.
E-mail: igounko@tcd.ie, Tel: +353-1-8963543

[c] St. Petersburg National Research University of Information Technologies, Mechanics and Optics, 197101, St. Petersburg, Russia.

[1] *these authors contributed equally to this work.*

1. Introduction

The role of the electrolyte is to transfer electrons from counter electrode (CE) to the working electrode (WE) of the dye sensitised solar cell (DSSC), in order to regenerate the oxidised dye to its ground state (Longo and De Paoli, 2003). Therefore, the electrolyte is an essential component of DSSCs and its development is particularly important for further progress and commercialisation of DSSCs. In order to achieve high cell power conversion efficiencies, the electrolyte has to fulfil certain criteria including appropriate viscosity, high diffusion coefficient, high electrochemical and thermal stability, low vapour pressure and ease of sealing (Wei, 2010; Wu et al., 2007a). Traditional DSSC technology generally uses volatile solvent based electrolytes (Nogueira et al., 2001; Nogueira et al., 2004). These electrolytes are characterised by low viscosities and high diffusion coefficients. However, the liquid electrolytes cause a number of problems during and after manufacturing that limit their applications. The main problems include leakage of electrolytes, corrosion of cells over time, high temperature instability and additional complexity in trying to contain liquids in a solar cell device during manufacturing (Lee et al., 2010a; Wang et al., 2003c; Wu et al., 2007b). These drawbacks, as well as the fact that the solvent electrolytes are quite aggressive and can permeate plastics, are serious obstacles for large-scale application of DSSCs and their integration into flexible polymer based structures (Ahmad et al., 2011; Bai et al., 2008). To resolve the above problems, alternative components such as ionic liquids (ILs) have been investigated as a replacement for volatile organic solvent based electrolytes. ILs have good chemical and thermal stability, negligible vapour pressure, non-flammability and high ionic conductivity (Matsumoto et al., 2001) and can be tailored to produce good performance with low toxicity (Ghavre et al., 2014). However, the power conversion efficiencies obtained with ionic liquids at AM 1.5 solar irradiance have been lower than those achieved with organic solvent-based electrolytes (Wang et al., 2003b). DSSC employing the N719 sensitizer and a pure PMII electrolyte without any other additives achieves low efficiencies of 0.6 % at 1 sun(Lee et al., 2010a). DSSC containing PMII with various concentrations of iodine (0.05 to 0.44 M) exhibit efficiencies of 0.7 to 1.7 % at a temperature of 20°C (Berginc et al., 2007). Reasonable power conversion efficiencies were obtained with ILs, for example a power conversion efficiency of 7.2 % with binary ILs electrolytes, i.e. 1-propyl-3-methyl-imidasolium iodide (PMII) and 1-ethyl-3-methyl-imidasolium tetracyanoborate (EMIB(CN)) (Kuang et al., 2007a) and 6.4 % with co-sensitization of two organic dyes (SQ1 and JK2) (Kuang et al., 2007b). A 7.4% power conversion efficiency was reached with a mesoscopic

solar cell employing the binary ionic liquid electrolyte composed of PMII and 1-ethyl-3-methylimidazolium tricyanomethanide with the ruthenium sensitizer Z-907Na(Wang et al., 2005). Graetzel et al have reported a solvent free electrolyte with a mixture of three types of ILs i.e. 1, 3-dimethylimidasolium iodide, 1-ethyl-3-methylimidasolium iodide and 1-ethyl-3-methylimidasolium tetracyanoborate. They have demonstrated power conversion efficiency up to 8.2 % in their work(Bai et al., 2008). However, the use of ILs still introduces the problem of sealing and electrolyte leakage issues. Replacing the liquid electrolytes in the DSSCs with a solid (Byrne et al., 2013) or gel/quasi-solid state electrolyte is expected to address these problems (Stathatos et al., 2004). Various approaches have been employed to prepare gel/quasi-solid state electrolytes for DSSCs (Lan et al., 2006; Lan et al., 2007; Suresh et al., 2011; Zhang et al., 2012). For example an electrolyte consisting of PMII and I_2 solidified with SiO_2 nanoparticles achieves efficiencies of 1.2 to 1.5 % (Berginc et al., 2008). Graetzel et al. (Wang et al., 2003a) reported the incorporation of nanoparticles of SiO_2 into IL (PMII) and they achieved 7 % power conversion efficiencies for both the liquid and the corresponding quasi-solid state electrolyte/DSSCs. The presence of SiO_2 had no adverse effect on the conversion efficiency and offers the advantage that these electrolytes are free from leakage issues. Other papers reported increased power conversion efficiencies after the incorporation of various carbon (e.g. carbon nanotubes or CNT) based materials into ionic liquid electrolytes/DSSCs (Brennan et al., 2011; Lee et al., 2010b; Usui et al., 2004) to form promising quasi-solid state electrolytes. However, the addition of graphene or carbon nanotubes to ionic liquids leads to an increase of viscosity of the electrolyte that results in the limited penetration into thick sensitised porous TiO_2 layers of working electrode (Ahmad et al., 2011). Therefore an optimisation both of ionic liquid-graphene or nanotube containing electrolytes and TiO_2 based working electrodes are necessary for further improvement of corresponding cell efficiencies.

In our previous reports we developed a series of carbon based quasi-solid state electrolytes for DSSC by the incorporation of either graphene, SWCNTs or a mixture of both SWCNTs and graphene into the ionic liquid PMII (Ahmad et al., 2011; Brennan et al., 2013). These electrolytes showed promising performance in DSSC, with optimised compositions found to be graphene (30 wt %) in PMII, SWCNTs (7 wt %) in PMII and 3 wt % SWCNT + 12 wt % graphene in PMII achieving efficiencies of 2.10 %, 1.43 % and 2.50 % respectively. Furthermore, these carbon nanomaterial filled electrolytes show good stability, still having much higher efficiencies than that of pristine PMII after 1000 hrs of aging. In an effort to

improve DSSC performance, we now present new results achieved with an optimised TiO_2 WE. Our DSSC fabrication procedure was improved by additional treatment of the WEs, incorporation of a scattering layer, optimising the thickness of TiO_2 layer and treatment with $TiCl_4$ to produce compact blocking layers, all of which combine to improve the quasi-solid state based DSSC performance considerably.

2. Experimental

2.1 General procedures

Powdered graphite was purchased from Branwell (Branwell natural graphite). 1-Methyl-3-propylimidasolium iodide (PMII) was purchased from Io-li-tec. SWCNTs were supplied by Elicarb (SWCNT, PR 0925, 10g). N-Methyl-pyrrolidone (NMP) was supplied by Sigma-Aldrich. Graphene samples were prepared according to the Khan et al. method (Khan et al., 2010a). Ultrasonic Bath Grant XB6 (200 W) was used in all sonication experiments.

2.2 Preparation of quasi-solid state electrolytes

The graphene samples were triturated in a vial and again dried in an oven for 4 hours at 65°C to remove the traces of NMP, if any remained in graphene powder. The graphene powder was dispersed in PMII at concentrations of 30 % by weight. Graphene was added in small portions to PMII, followed by sonication for 30 minutes. After this, samples were sonicated in closed glass vials in an ultrasonic bath for a further 4 hours until homogeneous quasi-solid state electrolytes were obtained. SWCNTs (7 wt %) were dispersed in PMII. The mixture was sonicated by an ultrasonic tip Bandelin Sonopuls HD 2200 at 20 % power for 10 minutes. Samples were then sonicated in an ultrasonic bath in closed glass vials for further 4 hours. Hybrid graphene and SWCNTs quasi-solid state electrolytes were prepared: with 12 % of graphene and 3 % of SWCNTs by weight dispersed in PMII. Samples were sonicated using an ultrasonic tip at 20 % power for 10 minutes and then sonicated in an ultrasonic bath for a further 4 hours.

2.3 DSSC fabrication procedure

The working electrodes in this study were prepared using the screen-printing method reported in (Kroon et al., 2007), which is based on a layer-by-layer deposition of TiO_2 on a fluorine doped tin oxide (FTO) conducting transparent glass substrate. Commercial grade materials are employed so that any findings may be transferred to industrial manufacturing

processes. In all cases a non-porous dense blocking under-layer of TiO_2 was deposited on the FTO substrate via $TiCl_4$ treatment (Ito et al., 2008) in order to reduce charge recombination. TiO_2 paste was then printed on the $TiCl_4$ treated glass using a TIFLEX Ltd. manual screen-printer and involved several cycles. After each TiO_2 paste deposition, the films were kept in an ethanol chamber for 6 mins followed by drying at 125 °C for 6 min, while the final sintering involved gradually heating in an oven at 325°C (5min), 375°C (5min), 450°C (15min), 500°C (30min). Following sintering the electrodes were again treated with $TiCl_4$ followed by sintering at 500°C for 30 mins. The TiO_2 active area was 0.28 cm^2 (consisting of a 6 mm diameter circular spot). The sintered electrodes were placed in a dye bath of N719 (DyeSol Ltd) dissolved in acetonitrile:tert-butylalcohol:THF (vol 4.5:4.5:1) for 16-20 hours. Dyes were procured from commercial suppliers and used without further purification. The counter electrode was prepared with a thin film of Pt catalyst deposited via a drop of H_2PtCl_6 solution (2 mg Pt in 1 ml ethanol) and heat treated at 400°C for 15 minutes to remove the solvent. The dye coated TiO_2 electrode and Pt coated counter electrode were sandwiched together with clips using a 50 µm Bynel polymer gasket/spacer. TiO_2 printing pastes employed were a "transparent" paste containing TiO_2 particles of average size 20 nm formed from P25 powder using the standard fabrication procedure reported in (Ito et al., 2007). Ethyl cellulose (Fluka, #46080 and #46070) and anhydrous Terpineol (Sigma-Aldrich, 86480) were used as received in making this paste. A "scattering" paste was purchased from DyeSol Ltd (WER 2-0) which contains titanium oxide particles of size in the range of 150 nm to 250 nm, formulated to provide an opaque white scattering layer. Both pastes were screen printed with a 90 T mesh and their thicknesses after sintering were measured with an optical profilometer. Three working electrode configurations were employed in this study (full details in Table 1). A working electrode (WE) without any scattering layer in a 6+0 configuration (6 transparent layers + 0 scattering layers, total thickness after sintering = 10 µm) is labelled WE A. A 7+2 electrode configuration (7 transparent layers + 2 scattering layers, total thickness after sintering = 15 µm) is labelled WE C. Details of the DSSC electrodes used in previous study are available here (Ahmad et al., 2011) and are labelled WE B. WE B electrodes (10 µm thick TiO_2 layer), counter electrode (Pt coated) and dye (N719) were supplied by Dyesol limited. WE B consisted of active-opaque titania films of TiO_2 formed using DSL 18NR-AO paste (Dyesol Ltd) containing 20 nm nanoparticulates and scattering particles of average size 350 nm to 450 nm. Sealant/spacer (Meltonix 1170-60 series) was purchased from Solaronix SA.

2.4 Characterisation of DSSC

Electrolyte performance in fully fabricated DSSC was investigated by measuring I-V curves. Illumination was provided by a solar simulator (Newport 91195A-1000) using a Newport 69920 Arc Lamp Power Supply yielding a 4 x 4 inch beam size. In order to simulate standard AM1.5 light conditions an Air Mass Filter (Newport 81088A) was placed before the output of the solar simulator. Irradiance powers were measured using a Newport 91150V Calibrated Reference Solar Cell. I-V measurements were recorded with a GAMRY Instruments Potentiostat at irradiance powers of 1000 W/m^2. We report the performance for the best performing cell in each case.

Electrochemical Impedance Spectroscopy (EIS) measurements were recorded with a GAMRY Instruments Potentiostat with a perturbation amplitude of 10 mV and frequency range between 10^5 and 10^{-1} Hz. A Gamry Instruments model editor Version 5.30 was used to create an equivalent circuit model. The model was used to fit to experimental data using the Gamry Echem Analyst Software. Symmetric cells composed of two Pt coated counter electrodes (CE) sandwiching a 50 µm thick Bynel spacer and containing the specified electrolyte were fabricated for EIS studies of the electrolyte materials and their charge transfer resistances at the CE interface (active area = 1 cm diameter circle (0.785 cm^2)). EIS of the symmetric cells was measured in the dark at open-circuit potential (0 V) (Liberatore et al., 2009).

Table 1: Description of working electrodes for DSSC

Parameter	**A**	**B**	**C**
Active Area	0.28 cm^2 (0.6 cm diameter circle)	0.8 cm^2 (1 x 0.8 cm rectangle)	0.28 cm^2 (0.6 cm diameter circle)
Thickness	10 µm	10 µm	15 µm
Scattering layer	No	No	Yes
Average Particle size(s)	P25: 20 nm	DSL 18NR-AO: 20 nm (70 %), 350-450 nm (30 %)	P25: 20 nm WER2-O: 150-250 nm
Description	Single layer: Transparent (10 µm)	Single layer: Active-Opaque (10 µm)	Double layer: Transparent (10 µm) + Opaque scattering layer (5 µm)
$TiCl_4$/ TiO_2 underlayer	Yes	No	Yes
$TiCl_4$/ TiO_2 overlayer	Yes	No	Yes

3. Results and discussion

3.1 Working electrode (WE) optimisation

The main aim of this study is to improve the photovoltaic performance of our previously reported carbon nanomaterial containing quasi-solid state electrolytes/DSSC (Ahmad et al., 2011) by optimising: thickness of TiO_2 layer, incorporation of TiO_2 scattering layer and also $TiCl_4$ treatment of WEs. In this work three optimised carbon based quasi-solid state electrolytes i.e., (1) graphene (30 wt %), (2) SWCNTs (7wt %) and (3) a mixture of graphene (12 wt %) and SWCNTs (3 wt %) were incorporated into 1-methyl-3-propylimidasolium iodide (PMII) according to our previous published report (Ahmad et al., 2011). A description of the types of WE employed in this study are listed in Table 1. The WE are labelled A, B and C respectively. WE A contains 20 nm particles of TiO_2 only, making the TiO_2 layer almost completely transparent. WE B contains an active–opaque layer of TiO_2 containing a random dispersion of TiO_2 particles of two different sizes (70 % of 20 nm particles and 30 % larger 400 nm light scattering particles). WE C is composed of a bi-layer structure, with a 10 µm thick transparent layer of TiO_2 (20 nm particle size) coupled with a 5 µm thick layer of scattering particles (~200 nm particle size). These electrode structures and their expected effects on incoming light are presented schematically in Fig. 1. Performance parameters of DSSCs fabricated with these three different electrode configurations and the optimised carbon nanomaterial containing quasi-solid state electrolytes are displayed in Table 2. Comparing results between electrode A (Fig. 2) and B, which both consist of same thickness of TiO_2 (10 µm), for all three electrolytes better photocurrent is observed for the working electrode B. Efficiency values are observed to increase from 1.21 % to 1.43 % (SWCNTs), 1.78 % to 2.50 % (SWCNT-graphene) and from 1.53 % to 2.10 % (graphene). WE B is the same thickness but contains 30 % scattering particles implying the use of scattering particles increases light capture within the cell for these quasi-solid electrolytes and is crucial for achieving better efficiencies. However, the presence of large particles near the conducting glass (WE B) can cause strong back-scattering of incoming light and unavoidably results in light loss (Wang et al., 2004).

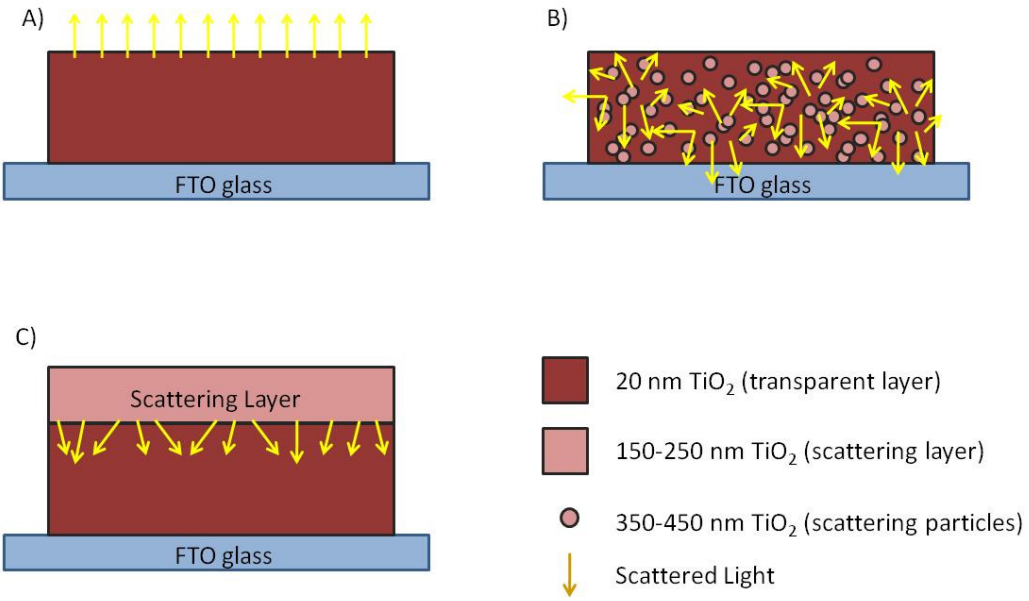

Fig. 1. Schematic representation of the working electrodes (WE) employed.

In an effort to improve performance further, cells were then fabricated using electrode configuration C in which scattering particles were incorporated with the bi-layer technique involving first a 10 µm thick transparent layer of 20 nm sized particles followed by a 5 µm thick layer of larger TiO_2 scattering particles. TiO_2 scattering particles in the bi-layer format are well known to improve DSSC performance by back scattering any light not absorbed by the active layer back through the cell, thus increasing light capture (Hore et al., 2006; Wang et al., 2004).

In the cases of SWCNT and hybrid (SWCNT-graphene) based quasi-solid state electrolytes, improved DSSC performance is observed with electrode C (Table 2, Fig. 3). Efficiency values increase from 1.43 % (SWCNTs) and 2.50 % (SWCNT-graphene) to 3.49 % and 2.93 % respectively. Improvements in all cell parameters of short-circuit current density (J_{sc}), open circuit voltage (V_{oc}) and fill factor (FF) are observed. The superiority of electrode configuration C can be rationalised in terms of the bi-layer scattering approach and that there is now no presence of large particles near the conducting glass, as in the case of WE B, and this loss mechanism is now avoided. Furthermore, WE C underwent additional surface treatments with a $TiCl_4$ solution before TiO_2 paste printing (underlayer) and again following TiO_2 paste printing (overlayer) in order to deposit a thin compact layer of TiO_2 particles on the surfaces. The underlayer reduces recombination at the FTO-electrolyte interface and improves interfacial adhesion between FTO and the nanoporous screenprinted

TiO_2 layer increasing V_{oc}, FF and J_{sc} (Choi et al., 2012). The overlayer results in more dye being adsorbed onto the oxide surface and a shift in the conduction band edge of the TiO_2 increasing the quantum efficiency of charge separation at the interface, thus causing an increase in photocurrent (Choi et al., 2012; O'Regan et al., 2007; Sommeling et al., 2006). Table 2 presents a summary of photovoltaic parameters including short-circuit current density (J_{sc}), open circuit voltage (V_{oc}), fill factor (FF) and power conversion efficiency of all quasi-solid state electrolytes investigated in this work. Unlike the SWCNT and hybrid (SWCNTs-graphene) electrolytes, in the case of the graphene electrolyte, a decrease in performance is observed from 2.10 % to 1.96 % upon changing from WE B to WE C. This may be related to the highly viscous, thick gel like nature of this electrolyte which inhibits its filling of the TiO_2 pores for the thicker 15 μm WE. This is also evidenced by the fact the hybrid electrolyte (SWCNTs-graphene) shows less performance increase with the thicker WE C.

Also of note is that the J_{sc} of the hybrid based quasi-solid state electrolyte (7.89 mA/cm^2) is higher than the SWCNTs based quasi-solid state electrolyte (7.35 mA/cm^2) indicating that the hybrid has higher conductivity. It has been previously reported in the literature that conductivity of the graphite/graphene composite can be increased by addition of small quantities of SWCNTs (Khan et al., 2010b). However, V_{oc} and FF of the hybrid is lower than the SWCNTs based electrolyte suggesting increased recombination and more resistance at the counter electrode. Details of which are studied using electrochemical impedance spectroscopy in Section 3.2.

Table 2: The photovoltaic parameters of DSSCs fabricated with various carbon nanomaterial containing quasi-solid state electrolytes with three different types of working electrode (WE). Full details of WE available in Table 1.

Electrolyte	**WE**	**Efficiency (%)**	**J_{sc} (mA/cm^2)**	**V_{oc} (mV)**	**FF**
SWCNTs(7 wt%) /PMII	A	1.21	5.00	560	0.43
	B	1.43	5.19	540	0.41
	C	3.49	7.35	711	0.67
Graphene (12 wt%) and SWCNTs (3 wt%)/PMII	A	1.78	6.70	580	0.45
	B	2.50	7.32	594	0.44
	C	2.93	7.89	640	0.58
Graphene(30 wt%)/PMII	A	1.53	5.21	580	0.50
	B	2.10	5.30	624	0.49
	C	1.96	6.89	600	0.47

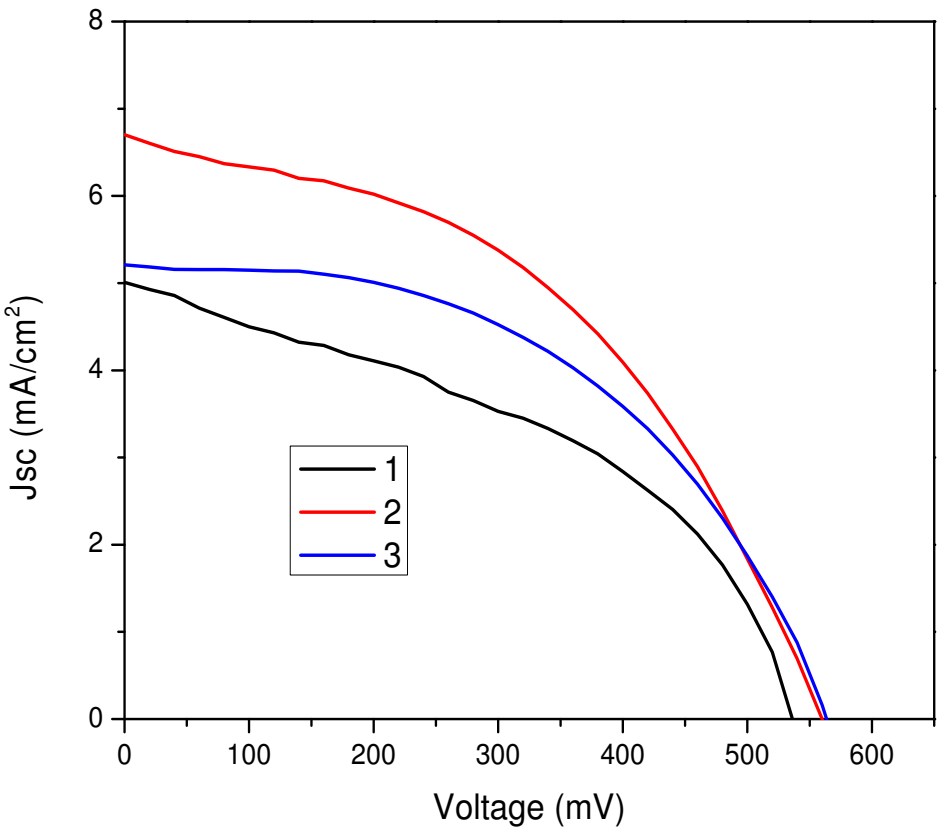

Fig. 2. The photovoltaic (J–V) curves of the quasi-solid state electrolytes/DSSCs with working electrode A and the following electrolyte: 1) SWCNTs (7 wt %), 2) Hybrid (SWCNTs 3 wt %+ 12 wt % graphene) and 3) Graphene (30 wt %).

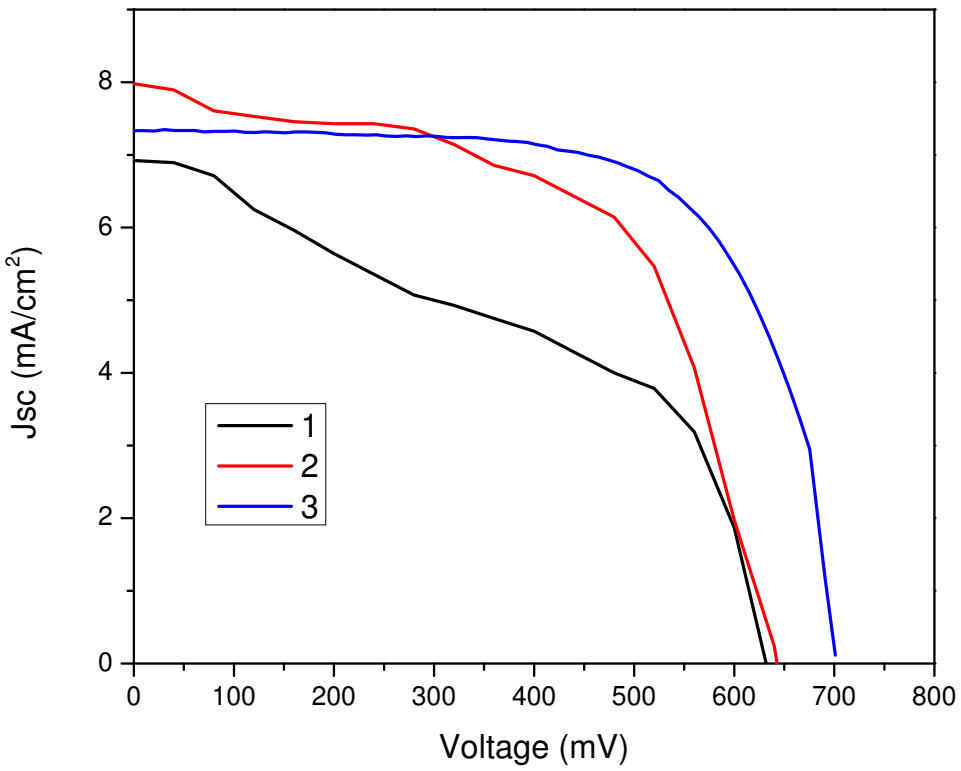

Fig. 3. The photovoltaic (J–V) curves of the quasi-solid state electrolytes/DSSCs with working electrode C and the following electrolyte: 1) Graphene (30 wt %), 2) Hybrid (SWCNTs 3 wt % + 12 wt % graphene) and 3) SWCNTs (7 wt %).

3.2 Electrochemical Impedance Spectroscopy (EIS)

In order to gain some insight into the charge transfer resistances of these electrolytes within the DSSC, particularly at the counter electrode-electrolyte interface, EIS spectroscopy was employed. Symmetric cells composed of our electrolyte sandwiched between two Pt based counter electrodes were fabricated and EIS measurements were performed. Symmetric cells such as this allow evaluation of the processes occurring at the Pt/electrolyte interface (Liberatore et al., 2009; Meng et al., 2014). The EIS Nyquist and Bode plots of the cells fabricated with the SWCNT and hybrid (SWCNT-graphene) electrolytes are shown in Fig. 4. Only one feature is present; symmetric cells allow assumption that identical reactions occur at the electrodes and that the single feature corresponds to charge transfer resistance at the Pt/FTO-electrolyte interface. The magnitude of the Bode plot peak for the hybrid electrolyte

is larger in magnitude than SWCNT electrolyte suggesting there is increased charge transfer resistance for the hybrid electrolyte (Kern et al., 2002). The Nyquist plot of the symmetric cells (Fig.4 (a)) can be used to evaluate the magnitude of the Pt/electrolyte resistances. The counter–counter symmetric cells are represented by the equivalent circuit shown in Fig. 4 of (Liberatore et al., 2009). The series resistance (Rs) represents the sheet resistance of the FTO glass, and is intrinsic to the transparent conducting oxide (TCO) glass itself. R1 represents the charge-transfer resistance at the electrolyte/Pt interface and a constant phase element (CPE) which represents an imperfect capacitor is introduced instead of capacitance because of the elevated porosity of the interface (Liberatore et al., 2009). A n value = 1 describes an ideal capacitor while the case n = 0 describes a pure resistor. In our case, the equivalent circuit can be simplified by assuming identical reactions at the electrodes, therefore yielding a single Randles-type circuit plus a series resistance as shown in the equivalent circuit inset of Fig. 4 (b), where R is the total resistance and the resistance at each CE/electrolyte interface is R/2. A Gamry Instruments model editor Version 5.30 was used to create the equivalent circuit and the data was fit using the Gamry Echem analyst Software. The resulting fitting of the Nyquist curve with this equivalent circuit yielded the electrolyte-counter electrode charge transfer resistance values shown in Table 3. As a reference, a cell using PMII electrolyte was also fabricated and large resistances almost 50 times the value of our novel electrolytes are observed indicating that PMII itself does not act as a good electrolyte (efficiency of only 0.16 % obtained with WE B; V_{oc} = 575 mV, J_{sc} = 0.37 mA.cm^{-2}, FF = 0.64). When PMII is doped with SWCNT or graphene the charge transfer resistance decreases significantly as seen from the much smaller sized semi-circles in the Nyquist plots and the lower calculated resistance values of 0.77-1.84 Ω (vs 67 Ω, PMII) hence the much better performance of these electrolytes compared to PMII on its own. Furthermore, these electrolytes show less resistance at the CE than organic solvent based electrolyte containing a redox couple and additives (34-37 Ω) (Liberatore et al., 2009).

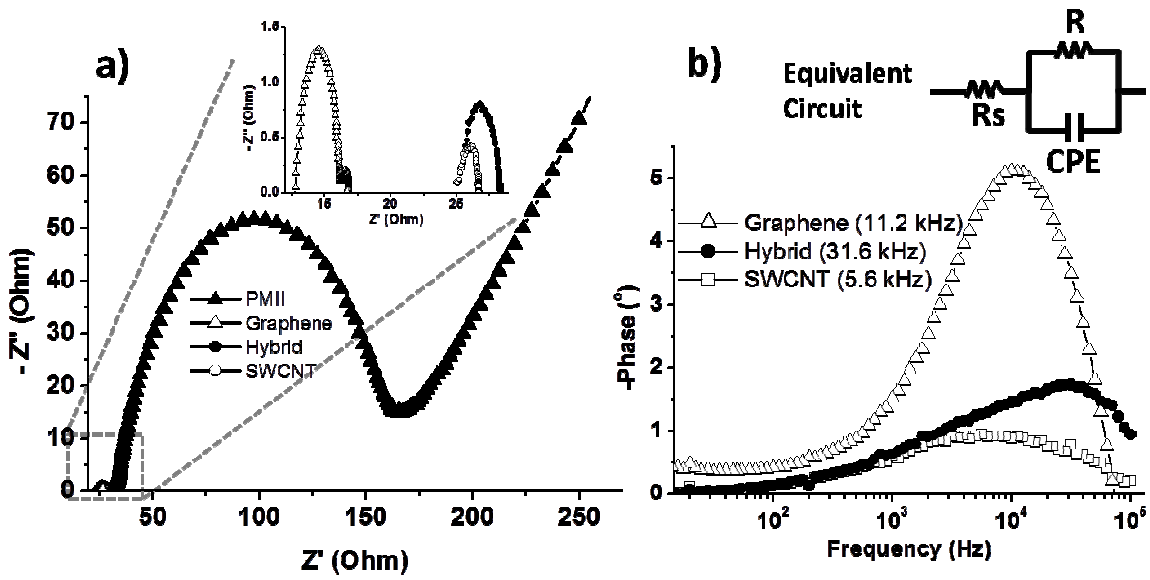

Fig. 4. EIS measurement data for CE-CE symmetric cells fabricated with the specified electrolyte. a) Nyquist plots, b) Bode plots, Inset - Equivalent circuit used for modelling the EIS data.

Table 3. Results of fitting the EIS data displayed in Fig. 4

Electrolyte	**Rs (Ohm)**	**R (Ohm)**	**n**	**$R_{CE\text{-}electrolyte}$ interface (Ohm)**
PMII	33.09 *±0.19*	133.8 *±1.16*	0.827 *±0.006*	66.9
SWCNT	25.18 *±0.36*	1.554 *±0.38*	0.690 *±0.201*	0.77
Hybrid (SWCNT + Graphene)	25.38 *±0.67*	2.994 *±0.70*	0.650 *±0.135*	1.49
Graphene	12.77 *±0.15*	3.683 *±0.17*	0.798 *±0.045*	1.84

The margin of error between the experimental data and the fits is presented in italics

4. Conclusions

In conclusion, in this work we have prepared and optimised the TiO_2 WE for our previously reported carbon nanomaterial containing quasi-solid state electrolytes for DSSCs. The power conversion efficiencies increased from 1.21 % (WE A: 10 µm, transparent) to 1.43 % (WE B: 10 µm, active opaque) to 3.49 % (WE C: 15 µm, bi-layer) for SWCNTs based quasi-solid state electrolyte/DSSC. The power conversion efficiencies of hybrid (SWCNT-graphene) based quasi-solid state electrolyte/DSSC increased from 1.78 % (WE A:

10 µm, transparent) to 2.50 % (WE B: 10 µm, active opaque) to 2.96 % (WE C: 15 µm, bi-layer). However, the power conversion efficiencies of graphene/PMII decreased from 2.10 % (WE B: 10 µm, active opaque) to 1.96 % (WE C: 15 µm, bi-layer) but remained higher than WE of same thickness without scattering particles (WE A: 1.53 % 10 µm, transparent).

These results reveal that relatively viscous graphene or hybrid (SWCNT-graphene) based quasi-solid state electrolytes give higher efficiency when thinner WEs (10 µm) are used while SWCNTs based quasi-solid state electrolytes are more efficient for thicker WE (15 µm). This suggests that highly viscous graphene or hybrid based quasi-solid state electrolytes cannot provide enough PMII penetration into thicker (15 µm) sensitised porous TiO_2 layer compared to thinner (10 µm) TiO_2 layer/WE. While SWCNTs based quasi-solid state compositions provide enough PMII penetration either into thinner or thicker sensitised porous TiO_2 layer/WE and thus show higher photovoltaic performance with thicker WE.

Electrochemical impedance spectroscopy (EIS) analysis demonstrates that the addition of SWCNT-graphene into PMII decreased the electrolyte-counter electrode charge transfer resistance (Rce) value from 67 Ω (only PMII) to 1.35 Ω. Which is almost 50 times lower than the Rce value for pure PMII. The Rce value was further decreased from 67 Ω (only PMII) to 0.88 Ω for SWCNTs based quasi-solid state electrolytes. We believe that the present results are very useful towards further development of new carbon based quasi-solid state electrolyte formulations for DSSCs and for the further improvement of the photovoltaic performance of corresponding carbon nanomaterial containing quasi-solid state electrolytes/DSSCs.

ACKNOWLEDGEMENTS

The authors would like to thank European Union (FP7 SMARTOP project, Grant Agreement number: 265769). K. R. T. acknowledges the SFI-Stokes Professorship grant support and award [S07/EN/E013]. I.A. and Y.K.G. would like to acknowledge the Irish Research Council for Science, Engineering & Technology (IRCSET) and SolarPrint Ltd. Y.K.G. acknowledges the Ministry of Education and Science of the Russian Federation (Grant No. 14.B25.31.0002) for financial support.

References

Ahmad, I., Khan, U., Gun'ko, Y.K., 2011. Graphene, carbon nanotube and ionic liquid mixtures: towards new quasi-solid state electrolytes for dye sensitised solar cells. Journal of Materials Chemistry, 21(42): 16990-16996.

Bai, Y. et al., 2008. High-performance dye-sensitized solar cells based on solvent-free electrolytes produced from eutectic melts. Nat Mater, 7(8): 626-630.

Berginc, M. et al., 2008. Ionic liquid-based electrolyte solidified with SiO2 nanoparticles for dye-sensitized solar cells. Thin Solid Films, 516(14): 4645-4650.

Berginc, M., Opara Krašovec, U., Jankovec, M., Topič, M., 2007. The effect of temperature on the performance of dye-sensitized solar cells based on a propyl-methyl-imidazolium iodide electrolyte. Solar Energy Materials and Solar Cells, 91(9): 821-828.

Brennan, L.J., Barwich, S.T., Satti, A., Faure, A., Gun'ko, Y.K., 2013. Graphene-ionic liquid electrolytes for dye sensitised solar cells. Journal of Materials Chemistry A, 1(29): 8379-8384.

Brennan, L.J., Byrne, M.T., Bari, M., Gun'ko, Y.K., 2011. Carbon Nanomaterials for Dye-Sensitized Solar Cell Applications: A Bright Future. Advanced Energy Materials, 1(4): 472-485.

Byrne, O., Coughlan, A., Surolia, P.K., Thampi, K.R., 2013. Succinonitrile-based solid-state electrolytes for dye-sensitised solar cells. Progress in Photovoltaics: Research and Applications: DOI: 10.1002/pip.2441.

Choi, H. et al., 2012. The effect of TiCl4-treated TiO2 compact layer on the performance of dye-sensitized solar cell. Current Applied Physics, 12(3): 737-741.

Ghavre, M. et al., 2014. Low toxicity functionalised imidazolium salts for task specific ionic liquid electrolytes in dye-sensitised solar cells: a step towards less hazardous energy production. Green Chemistry, 16(4): 2252-2265.

Hore, S., Vetter, C., Kern, R., Smit, H., Hinsch, A., 2006. Influence of scattering layers on efficiency of dye-sensitized solar cells. Solar Energy Materials and Solar Cells, 90(9): 1176-1188.

Ito, S. et al., 2007. Fabrication of screen-printing pastes from TiO2 powders for dye-sensitised solar cells. Progress in Photovoltaics: Research and Applications, 15(7): 603-612.

Ito, S. et al., 2008. Fabrication of thin film dye sensitized solar cells with solar to electric power conversion efficiency over 10%. Thin Solid Films, 516(14): 4613-4619.

Kern, R., Sastrawan, R., Ferber, J., Stangl, R., Luther, J., 2002. Modeling and interpretation of electrical impedance spectra of dye solar cells operated under open-circuit conditions. Electrochimica Acta, 47(26): 4213-4225.

Khan, U., O'Neill, A., Lotya, M., De, S., Coleman, J.N., 2010a. High-Concentration Solvent Exfoliation of Graphene. Small, 6(7): 864-871.

Khan, U., O'Connor, I., Gun'ko, Y.K., Coleman, J.N., 2010b. The preparation of hybrid films of carbon nanotubes and nano-graphite/graphene with excellent mechanical and electrical properties. Carbon, 48(10): 2825-2830.

Kroon, J.M. et al., 2007. Nanocrystalline dye-sensitized solar cells having maximum performance. Progress in Photovoltaics: Research and Applications, 15(1): 1-18.

Kuang, D. et al., 2007a. Stable, High-Efficiency Ionic-Liquid-Based Mesoscopic Dye-Sensitized Solar Cells. Small, 3(12): 2094-2102.

Kuang, D. et al., 2007b. Co-sensitization of Organic Dyes for Efficient Ionic Liquid Electrolyte-Based Dye-Sensitized Solar Cells. Langmuir, 23(22): 10906-10909.

Lan, Z. et al., 2006. Quasi-solid state dye-sensitized solar cells based on gel polymer electrolyte with poly(acrylonitrile-co-styrene)/NaI+I2. Solar Energy, 80(11): 1483-1488.

Lan, Z. et al., 2007. Quasi-solid-state dye-sensitized solar cells based on a sol–gel organic–inorganic composite electrolyte containing an organic iodide salt. Solar Energy, 81(1): 117-122.

Lee, C.-P., Chen, P.-Y., Vittal, R., Ho, K.-C., 2010a. Iodine-free high efficient quasi solid-state dye-sensitized solar cell containing ionic liquid and polyaniline-loaded carbon black. Journal of Materials Chemistry, 20(12): 2356-2361.

Lee, C.-P., Lin, L.-Y., Chen, P.-Y., Vittal, R., Ho, K.-C., 2010b. All-solid-state dye-sensitized solar cells incorporating SWCNTs and crystal growth inhibitor. Journal of Materials Chemistry, 20(18): 3619-3625.

Liberatore, M. et al., 2009. Using EIS for diagnosis of dye-sensitized solar cells performance. J Appl Electrochem, 39(11): 2291-2295.

Longo, C., De Paoli, M.-A., 2003. Dye-sensitized solar cells: a successful combination of materials. Journal of the Brazilian Chemical Society, 14: 898-901.

Matsumoto, H. et al., 2001. The Application of Room Temperature Molten Salt with Low Viscosity to the Electrolyte for Dye-Sensitized Solar Cell. Chemistry Letters, 30(1): 26-27.

Meng, K., Surolia, P.K., Byrne, O., Thampi, K.R., 2014. Efficient CdS quantum dot sensitized solar cells made using novel Cu2S counter electrode. Journal of Power Sources, 248(0): 218-223.

Nogueira, A.F., Durrant, J.R., De Paoli, M.A., 2001. Dye-Sensitized Nanocrystalline Solar Cells Employing a Polymer Electrolyte. Advanced Materials, 13(11): 826-830.

Nogueira, A.F., Longo, C., De Paoli, M.A., 2004. Polymers in dye sensitized solar cells: overview and perspectives. Coordination Chemistry Reviews, 248(13–14): 1455-1468.

O'Regan, B.C., Durrant, J.R., Sommeling, P.M., Bakker, N.J., 2007. Influence of the TiCl4 Treatment on Nanocrystalline TiO2 Films in Dye-Sensitized Solar Cells. 2. Charge Density, Band Edge Shifts, and Quantification of Recombination Losses at Short Circuit. The Journal of Physical Chemistry C, 111(37): 14001-14010.

Sommeling, P.M. et al., 2006. Influence of a TiCl4 Post-Treatment on Nanocrystalline TiO2 Films in Dye-Sensitized Solar Cells. The Journal of Physical Chemistry B, 110(39): 19191-19197.

Stathatos, E., Lianos, P., Surca Vuk, A., Orel, B., 2004. Optimization of a Quasi-Solid-State Dye-Sensitized Photoelectrochemical Solar Cell Employing a Ureasil/Sulfolane Gel Electrolyte. Advanced Functional Materials, 14(1): 45-48.

Suresh, S., Pandikumar, A., Murugesan, S., Ramaraj, R., Raj, S.P., 2011. Photovoltaic performance of solid-state solar cells based on ZnO nanosheets sensitized with low-cost metal-free organic dye. Solar Energy, 85(9): 1787-1793.

Usui, H., Matsui, H., Tanabe, N., Yanagida, S., 2004. Improved dye-sensitized solar cells using ionic nanocomposite gel electrolytes. Journal of Photochemistry and Photobiology A: Chemistry, 164(1–3): 97-101.

Wang, P. et al., 2005. Charge Separation and Efficient Light Energy Conversion in Sensitized Mesoscopic Solar Cells Based on Binary Ionic Liquids. Journal of the American Chemical Society, 127(18): 6850-6856.

Wang, P., Zakeeruddin, S.M., Comte, P., Exnar, I., Grätzel, M., 2003a. Gelation of Ionic Liquid-Based Electrolytes with Silica Nanoparticles for Quasi-Solid-State Dye-Sensitized Solar Cells. Journal of the American Chemical Society, 125(5): 1166-1167.

Wang, P., Zakeeruddin, S.M., Moser, J.-E., Grätzel, M., 2003b. A New Ionic Liquid Electrolyte Enhances the Conversion Efficiency of Dye-Sensitized Solar Cells. The Journal of Physical Chemistry B, 107(48): 13280-13285.

Wang, P. et al., 2003c. A stable quasi-solid-state dye-sensitized solar cell with an amphiphilic ruthenium sensitizer and polymer gel electrolyte [Erratum to document cited in CA139:182793]. Nature Materials, 2(7): 498.

Wang, Z.-S., Kawauchi, H., Kashima, T., Arakawa, H., 2004. Significant influence of TiO2 photoelectrode morphology on the energy conversion efficiency of N719 dye-sensitized solar cell. Coordination Chemistry Reviews, 248(13–14): 1381-1389.

Wei, D., 2010. Dye Sensitized Solar Cells. International Journal of Molecular Sciences, 11(3): 1103-1113.

Wu, J., Lan, Z., Lin, J., Huang, M., Li, P., 2007a. Effect of solvents in liquid electrolyte on the photovoltaic performance of dye-sensitized solar cells. Journal of Power Sources, 173(1): 585-591.

Wu, J.H. et al., 2007b. A Thermoplastic Gel Electrolyte for Stable Quasi-Solid-State Dye-Sensitized Solar Cells. Advanced Functional Materials, 17(15): 2645-2652.

Zhang, R.-K. et al., 2012. A new comb-like copolymer and its blend with poly(ethylene oxide) for solid electrolytes and application in dye-sensitized solar cells. Solar Energy, 86(9): 2346-2353.